Extended Abstract

The 4th Joint International Conference on Multibody System Dynamics
May 29 – June 2, 2016, Montréal, Canada

Kinematic Redundancy Resolution in Robotics and in Human Motion – An Experimental Case Study

Dóra Patkó[1] and Ambrus Zelei[2]

[1] *Department of Applied Mechanics, Budapest University of Technology and Economics, dora.patko94@gmail.com*
[2] *MTA-BME Research Group on Dynamics of Machines and Vehicles, zelei@mm.bme.hu*

The aim of this work is to gather information about humans' motion planning and experimentally find the artificial redundancy resolution algorithm adopted from the literatures [1, 2] which is the closest. The purpose is to get a little bit closer to understand the behavior of humans regarding the motion planning of the arm. Recently, redundancy resolution algorithms inspired by natural motion of humans or animals have captured the attention of many researchers. Such naturalistic motion is worth being designed in case of human-friendly robots, service and entertaining robots and humanoids. Experiences and measurement data may help to diagnostics of some musculoskeletal and/or nervous system's diseases, by comparing the motion of healthy control group and the diagnosed person. Knowledge about humans' natural motion planning may be also applied in physiotherapy.

We study the planar motion of the human arm augmented by a grasped bar, (see Fig. 1 left). The simplified mechanical model of the resulting three-link system and the interpretation of general coordinates $\mathbf{q} = [\varphi_1, \varphi_2, \varphi_3]^{\mathrm{T}}$ are depicted in the middle panel of Fig. 1. The coordinates of the endpoint can be uniquely determined by (1) as function of the joint angles q_i, which is called *direct kinematics*:

$$\mathbf{r}(\mathbf{q}) = \sum_{i=1}^{n} \left[L_i \cos(q_i), L_i \sin(q_i)\right]^{\mathrm{T}}, \tag{1}$$

where $n = 3$ is the number of links. In case of *kinematic redundancy* there are more degrees of freedom (DoF) than it would be minimally needed to carry out the prescribed task of a manipulator [1, 2]. The task is to follow a desired trajectory defined by the vector $\mathbf{r}^{\mathrm{d}}(t) = \left[x^{\mathrm{d}}(t),\, y^{\mathrm{d}}(t)\right]^{\mathrm{T}}$ thus the system is said to be kinematically redundant, because the dimensions of $\mathbf{r}^{\mathrm{d}} \in \mathbb{R}^2$ is smaller than the number of DoF = 3. In other words, the number of equations is fewer than the number of independent variables.

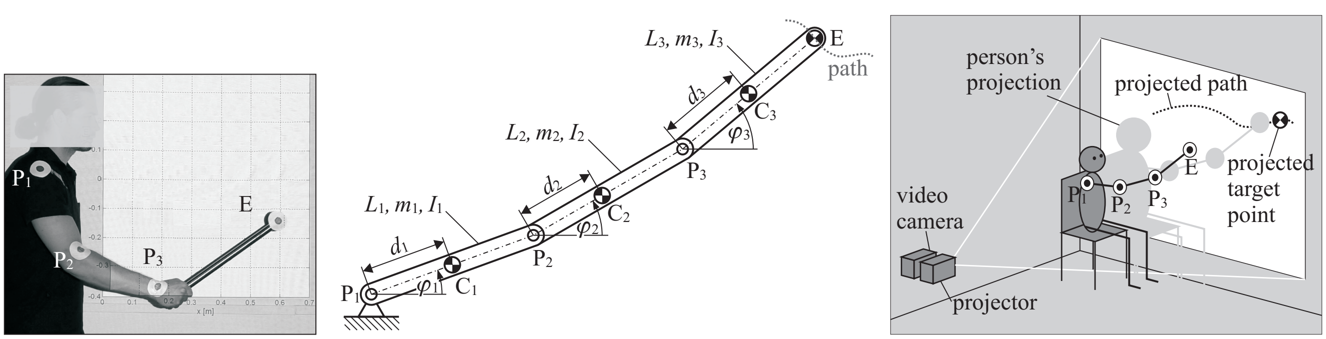

Fig. 1: Human arm augmented by a grasbed bar (left); Mechanical model of a 3DoF robotic arm (middle); Measurement setup (right)

We tested various solution methods for the *inverse kinematic* (IK) problem, when the unknown joint angles in $\mathbf{q}$ are to be calculated based on the inverse kinematics equation

$$\mathbf{r}(\mathbf{q}) - \mathbf{r}^{\mathrm{d}}(t) = \mathbf{0}. \tag{2}$$

The kinematic redundancy can be resolved by the augmentation of the IK equations (2). Virtual torsional springs are placed in the intermediary joints and their potential energy

$$U = \frac{1}{2} \sum_{i=1}^{n-1} s_i \left(q_{i+1} - q_i - \tilde{q}_{i+1}\right)^2 \tag{3}$$

is minimized, where s_i is the stiffness and $\tilde{q}_{i+1}$ is the preferred angle of link $i+1$ relative to link i. Equations $\partial U/\partial q_i = 0$; $i = 2\dots n-1$ augment the original set of IK equations (2). In this case, virtual springs are placed in the elbow (P_2) and the wrist (P_3). In method **a)** the resulting non-linear algebraic equation system is solved in closed form for uniform spring stiffnesses and zero preferred relative angles that leads to equal relative angles at the elbow and the wrist. In method **b)** each preferred relative angle was set to the middle of the joint limits of the shoulder, the elbow and the wrist (note: $\tilde{q}_1$ does not appear in (3)), which are $q_1 \in [-130°, 80°]$, $q_2 \in [-10°, 150°]$ and $q_3 \in [-30°, 30°]$ respectively [3]. The resulting algebraic equations are solved by Newton-Raphson method (NRM). As an alternative, the IK is resolved without the augmentation of equations (2) in **c)**. Instead, the *pseudo-inverse* (Moore-penrose generalized inverse) is used in the NRM to solve the non-unique problem in the form:

$$\mathbf{J}^{\dagger} = \mathbf{A}^{-1}\mathbf{J}^{\mathrm{T}}\left(\mathbf{J}\mathbf{A}^{-1}\mathbf{J}^{\mathrm{T}}\right)^{-1}, \tag{4}$$

where $\mathbf{J} = \partial\mathbf{r}/\partial\mathbf{q}$ is the Jacobian of (2) and $\mathbf{A}$ is an arbitrary weight-matrix, chosen to be an identity ($\mathbf{A} = \mathbf{I}$) in this approach. Approaches **a)**, **b)** and **c)** provide IK solution in geometric level, while the following methods utilize velocity level equations originated from (2) by time differentiation and from which the joint velocities can be expressed by using the pseudo-inverse again:

$$\mathbf{J}\dot{\mathbf{q}} - \dot{\mathbf{r}}^{\mathrm{d}} = \mathbf{0}, \tag{5}$$

$$\dot{\mathbf{q}} = \mathbf{J}^{\dagger}\dot{\mathbf{r}}^{\mathrm{d}} + \left(\mathbf{I} - \mathbf{J}^{\dagger}\mathbf{J}\right)\dot{\mathbf{z}}, \tag{6}$$

where the arbitrarily chosen vector $\dot{\mathbf{z}}$ is projected into the null-space of $\mathbf{J}$, so that it does not affect the endpoint's position but it can be used for optimizing the joint velocities $\dot{\mathbf{q}}$. After time integration of $\dot{\mathbf{q}}$, function $f = \dot{\mathbf{q}}^{\mathrm{T}}\mathbf{A}\dot{\mathbf{q}}$ will be minimized along the trajectory, if (4) is applied. Method **d)** uses $\dot{\mathbf{z}} = \mathbf{0}$ and $\mathbf{A} = \mathbf{I}$ substitutions and it provides the same trajectories as approach **c)**. In approach **e)**, the kinetic energy of the system is minimized, thus the pseudo-inverse is weighted by the mass matrix: $\mathbf{A} = \mathbf{M}$, and $\dot{\mathbf{z}} = \mathbf{0}$ is still used. The following methods minimize the scalar cost function g by using $\dot{\mathbf{z}} = k\,\partial g(\mathbf{q})/\partial\mathbf{q}$. Method **f)** ensures that the joint angles remain as close to the middle of the joint limits as it is possible by using the cost function: $g(\mathbf{q}) = \sum_{i=1}^{n}\left((q_i - q_i^{\mathrm{mid}})/(q_i^{\mathrm{mid}} - q_i^{\mathrm{max}})\right)^2$. Here q_i^{max} and q_i^{min} are the maximum and minimum limiting values of the ith joint range while the middle value is $q_i^{\mathrm{mid}} = (q_i^{\mathrm{max}} + q_i^{\mathrm{min}})/2$. Approach **g)** maximizes *manipulability* $\omega_{\mathrm{m}} = \sqrt{\det\left(\mathbf{J}\mathbf{J}^{\mathrm{T}}\right)}$ if the cost function is $g = -\omega_m$. Practically it means that the manipulator avoids singular values, when ω_m would be zero. The dynamic manipulability $\omega_{\mathrm{d}} = \sqrt{\det(\mathbf{J}(\mathbf{H}^{\mathrm{T}}\mathbf{H})^{-1}\mathbf{J}^{\mathrm{T}})}$ is maximized in method **h)** by choosing $g = -\omega_d$. $\mathbf{H} = \mathbf{W}\mathbf{M}$ includes a weight matrix $\mathbf{W} = \mathrm{diag}(1/\hat{\tau}_i)$, where $\hat{\tau}_i = \min(|\tau_i^- - g_i|, |\tau_i^+ - g_i|)$. The torque limits are τ_i^- and τ_i^+, while g_i is the torque of each link that compensates gravity. Method **h)** optimizes the ability to exert control force on the endpoint.

The simulation results obtained by the redundancy resolution algorithms **a)**-**h)** are compared with the measurement data obtained by video-capturing the motion of a large group of people. The inertial data and the estimation for the center of gravity position were provided by reference [4]. Each person had to follow a prescribed path with a pointer in their hands, while the joint angles were being recorded, as Fig. 1 shows. Three different tracking speeds and two different pointers with different mass were used in case of each person. In simulations, the robotic arm's endpoint E followed the previously measured path that was generated by the people. The deviation of each redundancy resolution method from the human motion was evaluated by using RMS error and statistical methods.

Acknowledgments: This work has been supported by the MTA-BME Research Group on Dynamics of Machines and Vehicles and by the Hungarian Scientific Research Fund, Hungary (OTKA) under grant numbers K-105433, K-101714 and PD-108691.

References

[1] J. M. Hollerbach and K. C. Suh, "Redundancy resolution of manipulators through torque optimization," *IEEE Journal of Robotics and Automation*, vol. 3, no. 4, pp. 308–316, 1987. DOI: 10.1109/JRA.1987.1087111.

[2] Y. Nakamura, *Advanced Robotics: Redundancy and Optimization*. Reading, MA: Addison-Wesley, 1991.

[3] F. Paulsen and J. Waschke, *Sobotta Atlas of Human Anatomy*, vol. 1. Elsevier GmbH, Munich, 15 ed., 2012.

[4] P. de Leva, "Adjustments to zatsiorsky-seluyanov's segment inertia parameters," *Journal of Biomechanics*, vol. 29, no. 9, pp. 1223–1230, 1996.